BRAIN
ORIGINAL ARTICLE

Giant axonal neuropathy: cross-sectional analysis of a large natural history cohort

Diana X. Bharucha-Goebel,[1,2] Gina Norato,[3] Dimah Saade,[1] Eduardo Paredes,[1] Victoria Biancavilla,[4] Sandra Donkervoort,[1] Rupleen Kaur,[1] Tanya Lehky,[5] Margaret Fink,[1] Diane Armao,[6,7] Steven J. Gray,[8] Melissa Waite,[4] Sarah Debs,[1] Gilberto Averion,[1] Ying Hu,[1] Wadih M. Zein,[9] A. Reghan Foley,[1] Minal Jain[4] and Carsten G. Bönnemann[1]

Giant axonal neuropathy (GAN) is an ultra-rare autosomal recessive, progressive neurodegenerative disease with early childhood onset that presents as a prominent sensorimotor neuropathy and commonly progresses to affect both the PNS and CNS. The disease is caused by biallelic mutations in the GAN gene located on 16q23.2, leading to loss of functional gigaxonin, a substrate specific ubiquitin ligase adapter protein necessary for the regulation of intermediate filament turnover.

Here, we report on cross-sectional data from the first study visit of a prospectively collected natural history study of 45 individuals, age range 3–21 years with genetically confirmed GAN to describe and cross-correlate baseline clinical and functional cohort characteristics.

We review causative variants distributed throughout the GAN gene in this cohort and identify a recurrent founder mutation in individuals with GAN of Mexican descent as well as cases of recurrent uniparental isodisomy. Through cross-correlational analysis of measures of strength, motor function and electrophysiological markers of disease severity, we identified the Motor Function Measure 32 to have the strongest correlation across measures and age in individuals with GAN. We analysed the Motor Function Measure 32 scores as they correspond to age and ambulatory status. Importantly, we identified and characterized a subcohort of individuals with a milder form of GAN and with a presentation similar to Charcot–Marie–Tooth disease. Such a clinical presentation is distinct from the classic presentation of GAN, and we demonstrate how the two groups diverge in performance on the Motor Function Measure 32 and other functional motor scales. We further present data on the first systematic clinical analysis of autonomic impairment in GAN as performed on a subset of the natural history cohort.

Our cohort of individuals with genetically confirmed GAN is the largest reported to date and highlights the clinical heterogeneity and the unique phenotypic and functional characteristics of GAN in relation to disease state. The present work is designed to serve as a foundation for a prospective natural history study and functions in concert with the ongoing gene therapy trial for children with GAN.

1 National Institutes of Health, Neuromuscular and Neurogenetic Disorders of Childhood Section, Bethesda, MD 20892, USA
2 Children's National Hospital, Division of Neurology, Washington DC, USA
3 National Institutes of Health, National Institute of Neurological Disorders and Stroke, Clinical Trials Unit, Bethesda, MD 20892, USA
4 National Institutes of Health, Rehabilitation Medicine Department, Bethesda, MD, USA
5 National Institutes of Health, EMG Section, Bethesda, MD 20892, USA

6   Department of Radiology, University of North Carolina School of Medicine, Chapel Hill, NC 27599, USA
7   Department of Pathology and Laboratory Medicine, University of North Carolina School of Medicine, Chapel Hill, NC 27599, USA
8   Department of Pediatrics, UT Southwestern Medical Center, Dallas, TX 75390, USA
9   National Institutes of Health, National Eye Institute, Bethesda, MD 20892, USA

Correspondence to: Carsten G. Bönnemann, MD
Neuromuscular and Neurogenetic Disorders of Childhood Section
Neurogenetics Branch, National Institute of Neurological Disorders and Stroke
NIH, Building 10, Room 2B39, 10 Center Drive, Bethesda, MD 20892-1477, USA
E-mail: bonnemanncg@nih.gov

Introduction

Giant axonal neuropathy (GAN) is an ultra-rare, autosomal recessive, progressive neurodegenerative disorder with onset in early childhood and death usually by the third decade. GAN results from mutations in the *GAN* gene, which encompasses 11 exons located on chromosome 16q23.2. Bilallelic disease-causing variants in *GAN* span the entire coding regions of the gene and include deletions, duplications, frameshift mutations, splice-site, missense and nonsense mutations.[1,2] GAN is caused by an abnormal or complete loss of function of gigaxonin, a broadly expressed Cul3 ubiquitin ligase substrate specific adaptor protein, which is normally present at extremely low levels in most cells throughout the body and strongly expressed in the brain, heart and skeletal muscle.[1,3–5] Gigaxonin comprises a BTB (Broad-Complex, Tramtrack and Bric a brac) domain, a Back domain and a Kelch Repeat domain. The BTB domain interacts with proteins involved in ubiquitination and protein chaperones, while the Kelch domain interacts with intermediate filaments targeted for degradation or turnover.[1,6] Gigaxonin is necessary for the regulation and appropriate turnover of intermediate filaments, so loss of function leads to progressive accumulation of native intermediate filaments affecting endothelial cells, skin fibroblasts, muscle fibres, Schwann cells, astrocytes and neurons.[5,7,8] The disease name derives from the pathological finding of 'giant' axons or axonal swellings, due to the abnormal accumulation of intermediate filaments within peripheral sensory and motor nerves, as well as in the CNS including: cerebral and cerebellar white matter, middle cerebellar peduncles, brainstem tegmentum, corticospinal tracts and posterior columns.[3,4,9–12] Dysregulated intermediate filaments in GAN include vimentin, desmin, cytokeratins, glial fibrillary acidic protein (GFAP), peripherin and neurofilaments,[5,6,11,13] causing neurodegeneration and neurologic disability. Abnormal intermediate filament inclusions have also been described in the myenteric plexus of the gastrointestinal tract, and are in keeping with clinical reports of symptoms such as constipation, reflux and vomiting seen in GAN, which supports the prospect of autonomic nervous system involvement in GAN.[6,14,15]

In typically affected individuals, early developmental milestones are normal, while tightly curled or 'kinky' hair due to abnormal accumulation of keratin[16] may already be evident. Onset is characterized by a decline in motor function, typically evident within the first few years of life. This is followed by progressive distal weakness of the upper and lower limbs often leading to a loss of ambulation by age 10 years or earlier.[17,18] GAN is a multisystemic disorder due to involvement of the central, peripheral and autonomic nervous systems. Its classic form involves weakness, impaired sensation, progressive dysarthria, dysphagia, impaired gastrointestinal motility, oculomotor apraxia, nystagmus, scoliosis, respiratory insufficiency and vision loss.[2,4,17] MRI provides a window into CNS disease showing progressive signal abnormalities distributed throughout the cerebrum, cerebellum and brainstem and, in many cases, notable spinal cord volume loss over time.[19–21] Here, it is important to note that, while this typical GAN phenotype and clinical findings are most prevalent, individuals with genetically confirmed GAN who are more mildly affected have also been reported. This milder form of GAN presents in children as an axonal Charcot–Marie–Tooth disease plus (CMT-plus) phenotype lacking many of the well-recognized systemic and CNS manifestations of 'typical' GAN, but with varying degrees of upper motor neurone findings that may include findings such as lower extremity spasticity or hyperreflexia. This axonal CMT-plus phenotype is becoming increasingly recognized and reported.[17,21–24]

Currently, there are no approved treatments for GAN beyond dedicated supportive care. A first in-human phase I clinical trial of intrathecal gene transfer for GAN has been initiated by us at the National Institutes of Health, NIH (NCT02362438). In support of this trial and future trials, it was essential to identify reliable and feasible outcome measures that are functionally relevant, capable of quantifying disease progression and useful for comparison to changes seen post-gene transfer. As follow-up visits are still in progress for the next few years, here we present the cross-sectional data from the initial visit in a single site natural history study for GAN. Our aims are to: (i) generate an overview of the genetic variants identified and explore possible genotype–phenotype correlations; (ii) characterize the baseline clinical signs and symptoms in individuals with GAN at various ages/stages of disease; (iii) identify reliable markers of disease severity; and (iv) assess how markers of disease severity correspond to ambulatory function and how they

are impacted by the classic versus milder phenotype. This cohort of 45 individuals with GAN aged 3–21 years represents the largest cross-sectional analysis performed thus far for GAN and serves as the baseline clinical and functional data for a longitudinal natural history assessment.

Materials and methods

Individuals with genetically confirmed GAN were enrolled and evaluated at the NIH. Written consent, and assent when applicable, was obtained from all individuals under study 12-N-0095, 'Clinical and Molecular Manifestations of Neuromuscular and Neurogenetic Disorders of Childhood', which has been approved by the National Institutes of Health Institutional Review Board (NIH-IRB Panel 1). Previous genetic testing records were reviewed to confirm eligibility. For those who did not have resolved genetic confirmation at the time of initial evaluation, sequencing and copy number variation analysis was performed in a CLIA (certified) laboratory and, when needed, parental testing was performed to confirm segregation of mutations. Medical histories and clinical evaluations were performed as part of the standard neurological evaluation.

A subset of individuals was distinguished *a priori* phenotypically in this study as clinically milder compared to the classic GAN phenotype based on the following motor characteristics: (i) maintained independent ambulation beyond 10 years of age; (ii) ambulation with assistance beyond 13 years of age; or (iii) ability to run and/or jump after 5 years of age. We define independent ambulation as the ability to walk 10 m without any assistance, including without orthotic devices and ambulation with assistance as the ability to walk 10 m using external support of a device, furniture or person.

Non-contrast 3 T MRI brain and spine were performed. We qualitatively rated the level of severity of the T_2 hyperintensity observed in the cerebral white matter and cerebellar white matter as well as the extent of spinal cord atrophy or thinning as follows: 0 = normal, 1 = mild, 2 = moderate, and 3 = severe.

Electrophysiological evaluations included sensory and motor nerve conduction studies. Compound motor action potential (CMAP) amplitudes and sensory nerve action potential (SNAP) amplitudes and conduction velocities were measured from the following nerves: median and ulnar motor and sensory nerves, peroneal motor and sural sensory nerves. The CMAP and SNAP amplitudes are reported here.

Pulmonary function measurements, performed in the spirometry laboratory, included forced vital capacity obtained in a seated position and are reported as percentage predicted values.

Autonomic function was evaluated in individuals within the scope of the natural history study, and the first recorded set of autonomic studies are presented here. Patient or parent report of autonomic dysfunction was measured using the Composite Autonomic Symptom Score (COMPASS) 31 self-assessment questionnaire, which comprises 31 questions that span across six domains of function: orthostatic intolerance, vasomotor, secretomotor, gastrointestinal, bladder and pupillomotor.[25] Quantitative assessments of autonomic function included: quantitative sudomotor axon reflex test (to assess Q-Sweat), heart rate response to deep breathing, tilt-table test, and Schirmer's test (to assess lacrimal secretion) (Supplementary material).[25,26]

Targeted composite scales administered included the Neuropathy Impairment Score (NIS) and the Friedreich Ataxia Rating Scale (FARS).[27,28] The NIS represents the summed scores of standard components of the neuromuscular clinical examination (strength, sensation and reflexes). In this study, we provide scores for each side and report the NIS as a total sum score of both sides, with a higher score representing greater neuromuscular impairment. The FARS is a scale validated for individuals with Friedreich's ataxia, comprising a sum score (maximum score 159) derived from evaluation of items including: neurological examination; activities of daily living; assessment of bulbar, upper and lower extremity function; rating of functional impact of ataxia and upright stability/gait tasks. We report on the total FARS score and on the FARS item 1 score (rating of functional impact of ataxia). Like the NIS, a higher score corresponds to more severe dysfunction.

Measures completed by a paediatric physical therapist include: impairment-based quantitative strength testing, functional capacity measured by the Motor Function Measure (MFM-32) and timed tests. Functional and strength methods and data are reported in the Supplementary material. MFM-32 is a 32-item standardized assessment of functional abilities such as rolling, sitting and standing. It has been validated in children and adults 6–60 years of age in congenital myopathies, congenital muscular dystrophies, Duchenne muscular dystrophy and various other neuromuscular disorders.[27,29–31] It measures motor capacity in three domains: D1 (standing and transfers) with a maximum score of 39, D2 (axial and proximal motor function) with a maximum score of 36, and D3 (distal motor function) with a maximum score of 20, for a total maximum score of 96. This scale is derived from the Gross Motor Function Measure (GMFM), which was previously evaluated in individuals with GAN.[17] MFM-32 directly corresponds to scores in GMFM,[32] and we therefore report here on the MFM-32 score and its subdomain scores. In participants under 6 years of age, the MFM-20, a shortened version of the MFM-32 accounting for developmental differences was administered. We report percentage scores calculated from the achieved score divided by the maximum score for each subdomain (D1, D2 and D3) as well as the total MFM-32.

Statistical design

Descriptive statistics on the cohort were conducted, using median and interquartile range (IQR) or n and percentage, as well as an overall description of clinical features. Spearman correlations were conducted on continuous variables to describe the relationship between variables at a single visit and were visualized using a correlation matrix, where each box represents the strength and direction of the correlation between each of the row/column measures. Age was visualized by ambulation status and tested using one-way ANOVA. MFM-32 was described visually by domain and overall, by ambulation status. NIS and FARS were also visualized compared to age and by ambulation status and investigated using Spearman correlation. Clinical outliers were also observed visually in scatterplots and several sensitivity analyses were run excluding this clinical subtype. MFM-32, NIS and FARS were also investigated by mutation type and tested using an independent samples t-test. Fisher's exact test was used to investigate sleep apnoea across ambulation groups, and pairwise tests were done and Bonferroni-adjusted. Relationships between forced vital capacity percentage score and functional outcome measures were tested with Spearman correlations, and between forced vital capacity and ambulation status with one-way ANOVA. Box plot figures display the median, 25th and 75th percentile values, and the whiskers demonstrate the relationship to the upper and lower limits as calculated using the IQR [e.g. upper limit defined as Q3 + 1.5(IQR)]. All tests were run at an α-level of 0.05. Analysis was performed using R v.3.5.3.

Table 1 Cohort characteristics

	Classic (*n* = 35)	Mild (*n* = 10)	Overall (*n* = 45)
Age, years			
Mean (SD)	8.7 (3.3)	12.7 (4.8)	9.6 (4.0)
Median [IQR]	7.9 [7.3, 10.8]	11.9 [8.8, 16.1]	8.8 [6.8, 11.4]
Range	3.2–19.0	7.3–21.3	3.2–21.3
Age <6 years, *n* (%) MFM 20 administered			
Yes	8 (23)	0 (0)	8 (18)
Sex, *n* (%)			
Male	18 (51)	2 (20)	20 (44)
Female	17 (49)	8 (80)	25 (55)
Race, *n* (%)			
American Indian or Alaskan Native	1 (3)	0 (0)	1 (2)
Asian	5 (14)	0 (0)	5 (11)
White	29 (83)	10	39 (87)
Black	0 (0)	0 (0)	0 (0)
Ethnicity, *n* (%)			
Hispanic	10 (29)	1 (10)	11 (24)
Non-Hispanic	25 (71)	9 (90)	34 (76)
Ambulation status, *n* (%)			
Independent	16 (46)	9 (90)	25 (56)
Assisted	9 (26)	1 (10)	10 (22)
Non-ambulant	10 (29)	0 (0)	10 (22)
Mutation, *n* (%)			
CRIM negative	14 (40)	0 (0)	14 (31)
CRIM positive	21 (60)	10 (100)	31 (69)

Demographic information as well as functional ambulation status shown in table, which includes a total of 45 individuals with GAN-s35 with the classic phenotype and 10 with the mild phenotype. Demographic information is noted as total number of patients followed by the percentage in parentheses. CRIM status refers to cross-reactive immunological material and is reported here as predicted CRIM status based on genetic phenotype. Those with biallelic null mutations are listed as CRIM negative, all others are listed as CRIM positive.

Data availability

The data that support the findings of this study are available from the corresponding author on reasonable request.

Results

Demographics

Forty-five individuals (56% female) with genetically confirmed GAN, age 3 to 21 years, were enrolled in the natural history study and evaluated at their enrolment visit. Thirty-five individuals had a phenotype consistent with the typical or classic GAN phenotype, and 10 had a milder clinical phenotype, according to the study definition (see 'Materials and methods' section). The cross-sectional cohort characteristic data from the first study visit are presented in Table 1.

Genetic analysis

Disease-causing variants in the *GAN* gene appeared to be evenly distributed throughout the gene, involving the BTB domain, Back domain and Kelch Repeat domain, without apparent 'hotspots'. Of 90 total alleles analysed in this cohort, 46 different pathogenic variants (mutations) in the *GAN* gene were observed, and included: missense mutations (53.3%), splice-site mutations (16.7%), frame-shifting deletions (15.6%), in-frame deletions (4%), nonsense mutations (7.8%) and whole gene deletions (2%) (Fig. 1 and Supplementary Table 1). Interestingly, five unrelated individuals in our series from non-consanguineous parents of Mexican heritage were homozygous for the same essential splice-site variant in intron 4 of the *GAN* gene (c.851+1G>A), probably representing a newly recognized founder mutation in this population. Two individuals had confirmed uniparental isodisomy (isoUPD), in both

cases causing homozygosity of the maternally inherited *GAN* variant. One individual was found to have possible paternal isoUPD, as she was homozygous for the paternally inherited variant and deletion testing was negative in that individual. Unfortunately, access to samples for further testing in this individual are not available.

Clinical phenotype

All individuals in this study exhibited clinical signs and symptoms of GAN, including curly or tightly curled (frizzy) hair (Fig. 2A and B), distal weakness and varying degrees of gait ataxia in the ambulant individuals. The mean reported age at symptom onset was 2.9 years, and motor development was typically reported as normal within the first year of life. The most commonly reported presenting symptom was abnormality in gait including an inconsistent and slapping quality gait with frequent falls (out of proportion to limb ataxia/dysarthria), suggesting an early predominantly sensory ataxia. Ambulatory status at the initial study visit was as follows: 10 non-ambulant, 10 requiring assistance to walk and 25 independently ambulant. Independently ambulant children (median age 7.3 years) appeared to be slightly younger than those who required assistance (median age 10.1 years) or were non-ambulant (median age 11.0 years), although this difference was not statistically significant [ANOVA $F_{(2,42)}$ = 3.09; P = 0.056] (Fig. 3). The mean reported age at loss of unassisted independent ambulation was 8.3 years (Supplementary Fig. 1).

Tightly curled (frizzy) or mildly curly hair was seen in all 45 individuals, and macrocephaly [head circumference > +2 standard deviations (SD) above the mean, or >98th percentile for age] was common (27/45; 60%) (Fig. 2A). Other commonly reported signs and symptoms reported in this GAN cohort include: reduced visual acuity (22/45; 49%), dysarthria (19/45; 42%), urinary abnormalities
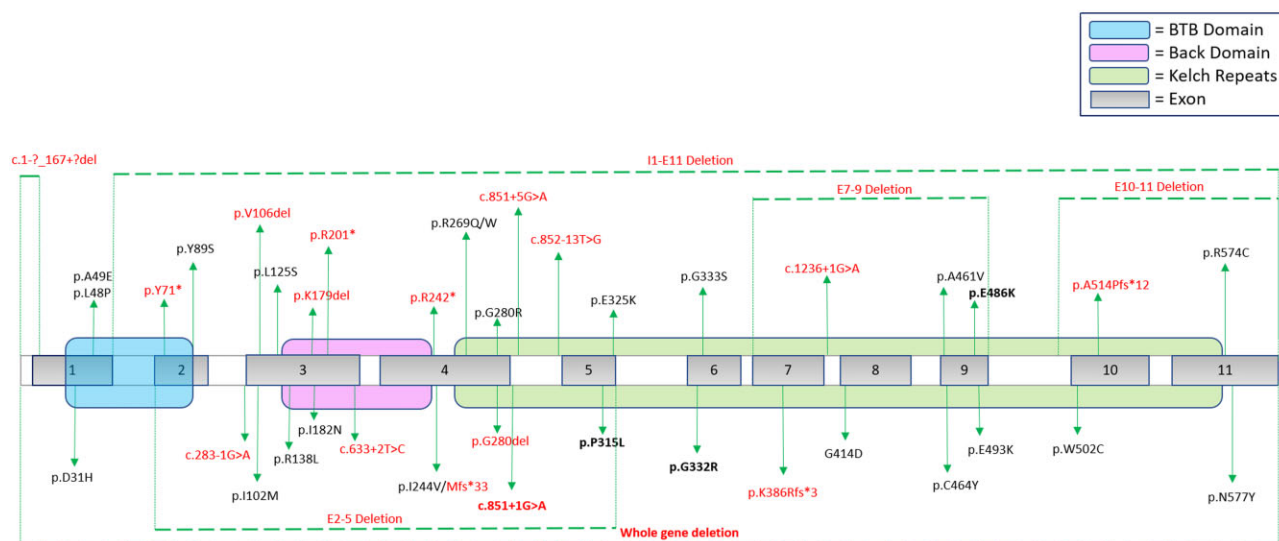
Figure 1 GAN mutations. Figure shows the *GAN* gene with mapping of the variants in our study cohort. Variants with deletions are noted with dashed lines above and below the gene map. Variants with predicted loss of function ('null' mutations) are shown in red. Variants that were recurrent in unrelated individuals in this study are highlighted in bold. Domains of the *GAN* gene are shown in colour including the BTB domain (blue), Back domain (pink) and Kelch Repeat domain (green).

(hesitancy or incontinence) (13/45; 28%), precocious puberty (11/45; 24%), illness associated hypothermia (5/45; 11%) and sleep apnoea (14/45; 31%) (Supplementary Table 2). Less commonly self-reported findings included vocal cord paralysis (*n* = 2) and stridor (*n* = 7). Orthopaedic manifestations include early joint contractures, foot deformities (including hammer toe deformity and cavovarus feet), toe walking and scoliosis. Finger contractures (Fig. 2C) were reported to begin with claw-like flexion contractures of the proximal interphalangeal joint in digits 4 and 5 and eventually progressed to involve other digits. Scoliosis was present at the initial study visit in 20/45 (44%) children, ranging in age from 5 to 15 years. Fig. 2D and E show the progression in scoliosis in a male with GAN at the ages of 12 and 15 years. Three children had spinal fusion surgery (ranging from 10–13 years) at the time of their first visit.

Other neurological manifestations reported included seizures (1/45; 2%), vertigo (11/45; 24%) and learning difficulties (12/45; 27%). Parental reports of school and learning difficulties were variable and ranged from attention deficit hyperactivity disorder to intellectual disability.

Gastrointestinal symptoms and signs commonly reported included: dysphagia (14/45; 31%), constipation (18/45; 45%) and lactose intolerance (18/45; 40%) (Supplementary Table 2 and Supplementary Fig. 2). Ten individuals have a reported history of episodic or recurrent vomiting, with 2 of the 10 having vomiting linked to intake of lactose. To our knowledge, in follow-up, three of the individuals within this cohort have had complications related to reduced gastrointestinal motility affecting refeeding following major surgery.

Neuroimaging

Of the 45 individuals evaluated, 37 completed a brain MRI and 41 individuals completed a spine MRI at the initial study visit. On brain MRI, cerebral and/or cerebellar white matter T_2 hyperintensities were frequently seen (28/37; 76%). The extent of severity of the white matter changes and atrophy qualitatively scored by brain MRI appear to correspond to other markers of disease severity, such as functional rating scales (MFM-32) (Supplementary Table 2). Neuroimaging abnormalities are progressive, as shown in Fig. 2G–J comparing brain MRI at 3 and 12 years of age in the same

individual (previous clinical MRI and study MRI, respectively). Early in disease, the distinctive increased T_2 signal abnormalities within cerebellar white matter surrounding the dentate nucleus of the cerebellum may be one of the earliest brain imaging findings in individuals with GAN and appears to precede the more widespread periventricular and deep white matter signal abnormalities associated with advanced disease. Cortical and spinal cord atrophy appear to correspond to more advanced disease severity and older age. Supplementary Table 2 reports on qualitative rating of the severity of periventricular and cerebellar white matter changes and spinal cord thinning.

Functional outcome measures

A correlation matrix (Fig. 4) was used to visualize the strength and frequency of correlations between variables studied in this GAN cohort. Individuals older than 6 years of age (*n* = 37) were used for this correlation matrix visualization, since normative data of strength are limited in children under 6 years (and where MFM-20 was administered instead). The total MFM-32 percentage score correlates significantly (either inversely or positively) with most of the variables studied, including age, NIS, FARS, proximal and distal strength, timed mobility and CMAP amplitude. The D1 (standing) and D2 (proximal) subdomains of the MFM-32 score correlate significantly with most other measured variables; however, the D3 (distal) domain does not correlate with timed ambulatory assessments. NIS and FARS composite scales correlate across most other tested variables, except the FARS does not appear to correlate well with timed ambulatory testing measures or proximal strength. Overall, the timed ambulatory assessments do not correlate with other measured variables including the composite scales (except for MFM-32 total percentage score), CMAP amplitudes and measures of strength, with the notable exception of knee flexion. Further breakdown of the MFM-32 scales (Fig. 5) shows the distribution of the total MFM-32 percentage score and the three subdomain scores (D1, D2 and D3) along with respective ambulatory status. The D1 and D3 domains are distributed across the range of scores from more severe to milder. The D1 performance is much more variable for independent ambulators, whereas D3 is more variable for those individuals who require assistance for
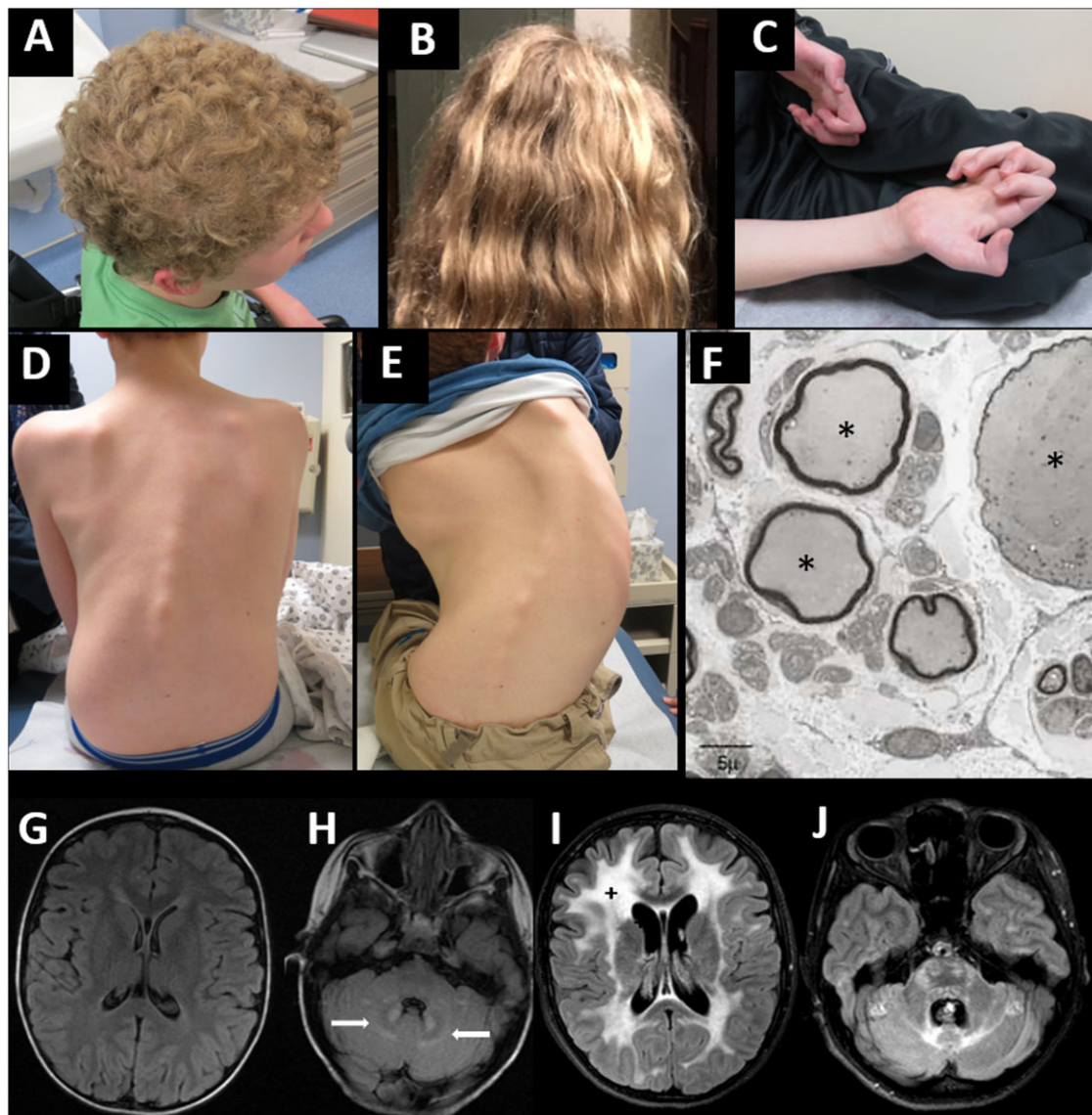
Figure 2 Clinical manifestations of giant axonal neuropathy. (**A**) Tightly curled (also classically described as 'kinky' or 'frizzy') hair in GAN—characterized by a dull appearance and course texture with tight curls. (**B**) Curly, but not 'frizzy' hair is seen commonly in those with milder disease severity (axonal CMT-plus phenotype). (**C**) Severe finger flexor contractures develop as seen here in a 15-year-old male with GAN. (**D** and **E**) Rapid progression of rotational and S-shaped scoliosis in the same male with GAN at age 12 years (**D**) and 15 years (**E**). (**F**) Enlarged (giant) axons (asterisks) surrounded by abnormally thin myelin sheaths on electron microscopy from a prior diagnostic sural sensory nerve biopsy in a child with GAN. (**G** and **H**) Axial FLAIR brain MRI in a 3-year-old female with GAN showing no significant signal abnormalities within cerebral white matter and early hyperintense signal abnormalities within cerebellar white matter in the region surrounding cerebellar nuclei (white arrows) as compared to (**I** and **J**) axial FLAIR brain MRI in the same female at 12 years of age showing confluent hyperintense signal abnormalities within the white matter (plus signs) of the cerebrum, cerebellum and brainstem.

ambulation or who are non-ambulant. D1 and D3 domains demonstrate the ability to discriminate by ambulation status, but not so for the D2 domain. This supports the clinical observation that proximal function is preserved longer in individuals with GAN, and therefore appears less impacted in ambulant as well as some non-ambulant individuals.

When analysing the total cohort, MFM-32 percentage score, NIS, and FARS composite scores do not correlate significantly with age (Fig. 4). However, when individual composite scores of functional assessment (MFM-32, NIS and FARS scores) are plotted against age and ambulatory status (Fig. 6), the individuals identified *a priori* in this study as belonging to the milder GAN phenotype (Fig. 6, data-points circled in grey) appear as outliers with better functional performance compared to similarly aged

patients with the classic GAN phenotype. Looking at the relationship between composite scores and age after exclusion of the individuals with mild phenotype (*n* = 10), we see highly significant Spearman correlations for all three scores (MFM-32: –0.71; NIS: 0.70; FARS: 0.78; all *P* < 0.001). As shown also in Fig. 6, the composite scores track well with ambulatory status and; therefore, they may be relevant markers of function for the classic GAN phenotype. Younger individuals with GAN (those <6 years of age) were evaluated with MFM-20 (not MFM-32). Given a limited number of children assessed by MFM-20 (*n* = 8), further conclusions about the performance of MFM-20 or correlation between MFM-20 and age cannot be made at this time (Supplementary Fig. 3).

When mutation consequence is taken into account, by designating patients as either predicted 'cross-reactive immunologic
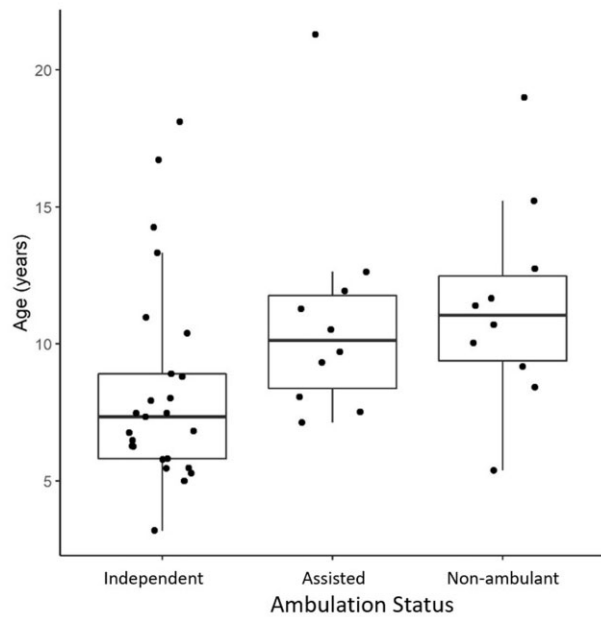
Figure 3 Ambulatory status compared to age. Box plot of ages in those who maintain their ability to walk independently, who walk with assistance and who have lost independent ambulation. Box plots represent the 25th and 75th percentiles within each group, and whiskers demonstrate the relationship to the upper and lower limits as calculated using the IQR [e.g. upper limit defined as Q3 + 1.5(IQR) or lower limit defined as Q1 – 1.5(IQR)]. Median age within each group is as follows: independently ambulant = 7.3 years, ambulant but requiring assistance = 10.1 years, and non-ambulant = 11.0 years.

material' or CRIM negative (if they have biallelic null mutations in the *GAN* gene), or predicted CRIM positive (if they carry at least one variant that is expected to result in some protein expression—missense or some splice variants), MFM-32, NIS and FARS appear to be impacted by the CRIM status (Fig. 7), with each group presenting with significant differences in performance (t-tests: MFM: $t = 3.3$; $P = 0.003$; NIS: $t = 2.86$, $P = 0.008$; FARS: $t = 3.33$, $P = 0.01$). Individuals with a mild phenotype, axonal CMT-plus, are circled in grey and removal of these outliers results in non-significant differences in the functional scales between the two genetic subtypes, suggesting that outside from the impact of mild GAN phenotype individuals in the CRIM-positive group, the classic manifestation of GAN appears to be similar between predicted CRIM-positive and predicted CRIM-negative individuals.

Pulmonary function

Respiratory involvement including worsening nocturnal hypoventilation or sleep apnoea occurred in those patients with more advanced disease. The presence of reported sleep apnoea was significantly related to ambulation type (assisted, non-ambulant or ambulant) (Fisher's exact, $P = 0.005$). Specifically, pairwise comparisons (Bonferroni-adjusted) show that the non-ambulant group is significantly more likely to have sleep apnoea than the independently ambulant group (6/10 versus 3/25; $P = 0.017$). Forced vital capacity (FVC) percentage (%) predicted score correlated well with key functional outcome measures (MFM-32: 0.54, $P = 0.002$; NIS: –0.53, $P = 0.003$; FARS: –0.48, $P = 0.01$; Spearman correlations). While FVC% did not correlate with timed ambulatory assessments, it did correlate with ambulatory status [ANOVA $F(2,26) = 6.28$, $P = 0.006$], with independently ambulant individuals having better performance than the non-ambulant group (Tukey's honestly significant difference $P = 0.02$).

Neurophysiology

Nerve conduction study data overall showed a length-dependent axonal sensorimotor polyneuropathy with significantly diminished CMAP and SNAP amplitudes and secondary demyelination leading to mild to moderate slowing of conduction velocities. Consistent with the clinical progression of the disease, sensory nerve responses were affected earlier than motor responses and were frequently absent as follows (where *n* refers to number of individuals where sensory response was evaluated): median sensory response absent in 50% ($n = 32$), ulnar sensory response absent in 57% ($n = 21$), and sural sensory response absent in 78% ($n = 27$). In contrast, motor responses (in upper extremity or proximal sites) were detectable and present in nearly all individuals, and therefore could be reliably obtained and correlated to other measures of function and strength in the cohort. As seen in the correlation plot, the median CMAP amplitude correlated significantly with other upper extremity measures of strength including grip and pinch strength (Fig. 4). In the lower extremity, peroneal CMAP amplitudes correlated to lower extremity strength measures (percentage predicted strength/myometry in knee flexion, knee extension and hip abduction) (Fig. 4). Overall, upper extremity CMAP amplitudes correlated significantly to the MFM-32% score and the total NIS score and can be reliably obtained across the spectrum of disease and, therefore, they appear to be the best electrophysiological measures to follow over time.

Autonomic function analysis

Evaluations of autonomic nervous system function were performed in a subset of individuals in this study and we report on the first time point of autonomic assessment, including: the COMPASS 31 autonomic symptoms questionnaire as well as targeted testing of sweat production, tear production and control of heart rate and blood pressure. The COMPASS 31 was completed in 14 individuals, and the domains with the highest frequency of reported abnormality were found within the gastrointestinal (78.6%), vasomotor (57.1%) and pupillomotor domains (57.1%) (Supplementary Fig. 2A). The average total weighted score was 13.14, range 2.11–40.19 (normative range: 10.2 ± 8.9).[33] Schirmer's test of lacrimal production was completed in 21, analysed in 20 individuals (one patient was excluded because of concomitant medication that may interfere with lacrimation). There appeared to be relative symmetry in the extent of lacrimation measured between eyes in the same individual, and we therefore report here on lacrimal secretion in the right eye (oculus dexter). Average measured lacrimation was 10.8 mm, range 0–35 mm and 12 individuals (60%) had moderate to severe reduction in appropriate tear production, while eight individuals (40%) had normal tear production (normal > 15 mm).[34] Q-Sweat was successfully completed in 11 individuals. The average volume of sweat yield in the upper extremity was 0.106 μl (range 0–0.510 μl) and in the lower extremity was 0.205 μl (range 0–1.207 μl). This is lower compared to healthy male paediatric patients between 5–18 years of age in whom the average forearm Q-Sweat volume was 0.65 ± 0.44 μl/mm²,[35] and also lower than the reported fifth percentile lower limit of normal in adults (0.14 μl female; 0.62 μl male).[25] The COMPASS 31 total weighted score and the Q-Sweat volume, while both abnormal, did not correlate significantly with age or the MFM-32 total score (Supplementary Fig. 2B–E). Only a small number of individuals of the cohort were able to complete the cardiovascular associated autonomic testing, which included tilt-table testing ($n = 8$) and assessment of heart rate variability with deep breathing ($n = 3$). During tilt-table testing, the increase in heart rate ranged from 4 to 27.6 beats per minute (bpm) (abnormal for postural orthostatic tachycardia is defined as an increase > 40 bpm) and there was no
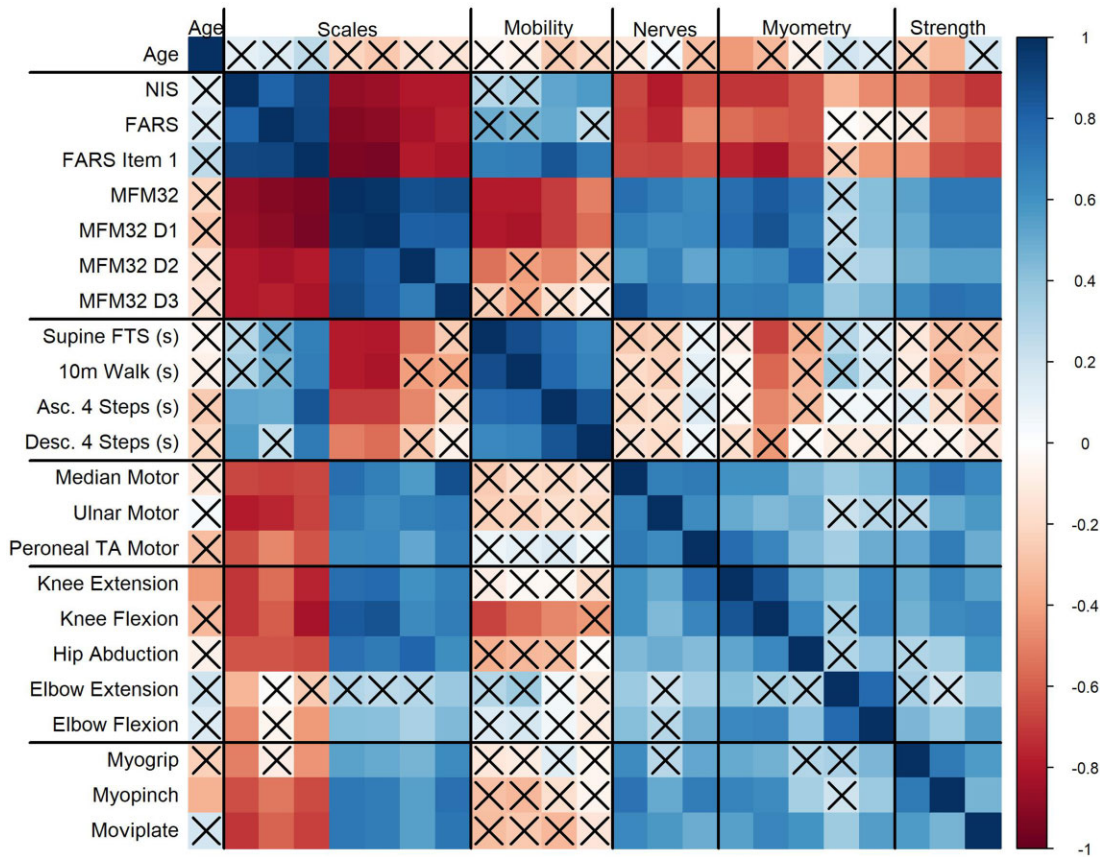
Figure 4 Correlation matrix. Correlation plot showing Spearman correlations using a continuous colour scale with positive correlations in blue and negative correlations in red (as shown in the bar to the *right*), and with a bolder colour representing a larger magnitude correlation coefficient. Outcome measures are duplicated in both the *x*- and *y*-axes, but along the *x*-axis, the variables are labelled only by overall clinical assessment type. Correlations between pairs of variables can be read by tracing across *x*- and *y*-axes in a grid format. Non-significant correlations are denoted with an X. This figure only uses data from 37 individuals (as these individuals were >6 years old). Clinical assessment types in the correlation matrix: Function: NIS, FARS, MFM-32 percentage score. Timed Testing: supine floor-to-standing (time to arise from lying supine on the floor to standing up); the time it takes to run 10 m, climb up four steps or descend four steps is also recorded. Nerves: median motor (recorded at abductor pollicis brevis), ulnar motor (recorded at abductor digiti minimi), and peroneal motor (recorded at the tibialis anterior muscle). Of note, the peroneal motor response was recorded from the tibialis anterior (TA) muscle, given that the more distally evaluated motor response from the extensor digitorum brevis was undetectable in many of the participants. Myometry: measure of percentage predicted value for the muscle groups/movements listed. Distal: myogrip [measure of grip force (kg) as compared to normative values]; myopinch [measure of pinch force (kg) generated with pinch task], and moviplate (number of finger taps between two objects).

observed drop in blood pressure. Thus, there did not appear to be a quantifiable abnormality in vasomotor response to position change. Heart rate response to deep breathing testing was limited in this study because of patient cooperation related to age and pulmonary function. In this study, heart rate response to deep breathing testing showed the difference between minimum and maximum heart rate ranged from 12.5 to 32.7 bpm, which is comparable to healthy controls where the average heart rate differences between minimum and maximum heart rate were 31.9 ± 11.3 bpm in children under 10 years of age and 25.7 ± 9.1 bpm in children over 10 years of age.[36] Heart rate variability with deep breathing did not appear to correlate to the vasomotor domain score on the COMPASS 31 scale (data not shown; Spearman correlation coefficient –0.61, $P = 0.58$) and, likewise, orthostatic intolerance as measured by rise in heart rate by tilt-table testing did not appear to correlate with the orthostatic domain of the COMPASS 31 scale (data not shown; Spearman correlation coefficient –0.19; $P = 0.65$).

Milder giant axonal neuropathy phenotype

We clinically identified 10 individuals (two full siblings) with a milder disease progression including a more prolonged preservation of ambulatory function than would be expected in the classical phenotype of GAN. They ranged in age from 8–21 years at the time of their first study visit, and the reported onset of symptoms was delayed in this group (average 5.4 years, compared to 2.3 years in classic GAN). Shared features among the milder individuals included: (i) at least one missense mutation in the *GAN* gene and predicted CRIM-positive status; (ii) minimal to no white matter changes or atrophy on brain MRI; and (iii) mildly curly rather than tightly curled hair [observed in 7/10 individuals with a milder GAN phenotype (Fig. 2B), while the other 3/10 had tightly curled (frizzy) hair]. Overall, these patients phenotypically are best characterized as axonal CMT-plus (Supplementary Table 1), with a more prominent polyneuropathy and less CNS and systemic involvement by imaging and clinically compared to classic GAN patients. Interestingly, 6 of the 10 milder GAN patients had at least one of the following signs of upper motor neurone involvement: lower extremity spasticity (and/or a spastic-ataxic gait pattern), hyperreflexia of the patellar deep tendon reflex or an extensor Babinski response. Of
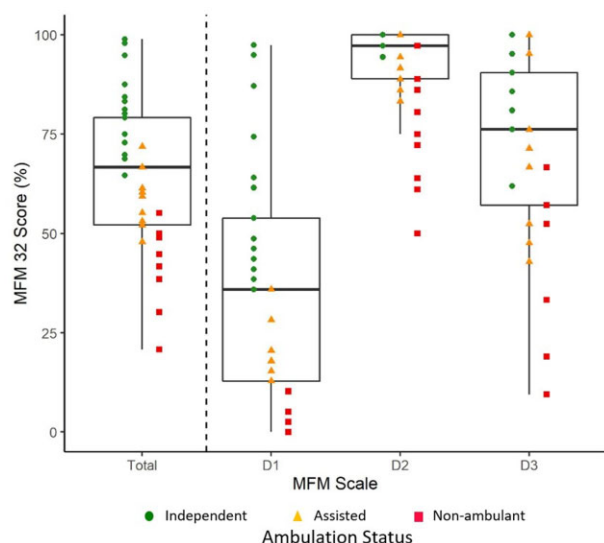
Figure 5 Ambulation status by MFM-32 score and subscale. Ambulation status by MFM-32 total percentage score and the MFM-32 subdomain (D1, D2 or D3) percentage scores are plotted. This plot only includes individuals over the age of 6 where MFM-32 was performed (n = 37). Eighteen individuals were independently ambulant, 10 required assistance to walk, and nine were non-ambulant (as indicated by the coloured shapes). Each individual's total score and subscale score are plotted. The box plots highlight the MFM-32 total percentage score as well as the percentage score for the subdomains with scores as follows [median (25th percentile; 75th percentile)]: MFM-32 total, 64.5 (52.10; 79.17); D1, 35.55 (12.82; 53.85); D2, 91.21 (88.9; 100); D3, 72.46 (57.1; 90.5). Whiskers reflect relationship to the upper and lower limits as calculated using the IQR [e.g. upper limit defined as Q3 + 1.5(IQR) or lower limit defined as Q1 – 1.5(IQR)]. The MFM-32 total score, D1 score and the D3 score are distributed across the range of scores from more severe to milder, while the D2 domain appears to show a possible ceiling effect, with a lower D2 score not seen until individuals have lost ambulation.

the remaining four milder GAN patients, three had normal neuroimaging and one had mild white matter abnormalities seen in the cerebellar white matter. Objectively, those individuals who are identified as having a milder GAN phenotype scored higher on the MFM-32 scale compared to those with the classic GAN phenotype of similar age (Fig. 7). The average total MFM-32 percentage score in the milder GAN cohort was 88.9 (range 75–100), whereas in the classic cohort the average was 52 (range 13–80). The presence of individuals with the milder GAN phenotype within this cohort affects the significance of the correlation between age on variables such as NIS, FARS and MFM-32 score. Looking again at results of analysing ambulatory status by age (Fig. 3), if we reanalyse these data excluding the mild phenotype, we see a much stronger relationship [ANOVA $F(2,32) = 13.38$; $P < 0.001$]. We also see a difference between the mild and classic GAN phenotype subgroups in ambulatory ability (Table 1). Overall, the presence of the milder GAN phenotypic subgroup and the way it confounds potentially important findings may be useful to consider for future trials.

Discussion

We report here on the baseline cohort characteristics and assessments from an ongoing longitudinal natural history study for individuals with GAN. We evaluated 45 participants with genetically confirmed GAN and present cross-sectional clinical, imaging and functional data from their first study visits. In the classic phenotype of GAN, we find a mean reported age of onset of gait or motor impairment at 2.3 years of age, a consistent finding of tightly

curled hair and a high frequency of associated medical symptoms affecting speech, swallowing and respiratory function as well as associated scoliosis, joint contractures, gastrointestinal issues and in some cases learning difficulties. The average reported age of loss of independent ambulation was 8.3 years old in the entire GAN study cohort. In contrast, we report on 10 individuals in this series who are milder, with an axonal CMT-plus phenotype. Genetically, all milder GAN patients had at least one missense variant in the GAN gene, with the missense variants distributed throughout the GAN gene. Interestingly, one compound heterozygous missense variant, p.P315L in exon 5 (within the Kelch Repeat domain of the GAN gene) was found in three unrelated patients with mild GAN.

The reported mean age of onset of symptoms in this axonal CMT-plus GAN subcohort was 5.4 years old. These patients predominantly exhibit distal weakness, unsteady or ataxic gait, and, in some, lower extremity spasticity. These milder patients tend to have curly rather than tightly curled hair. While patients with the classic form of GAN typically exhibit brain MRI changes including bilateral, symmetric, confluent areas of white matter T_2 signal intensity (characteristic of genetic/metabolic disorders affecting the CNS), individuals with the milder GAN phenotype tend to lack these findings on brain MRI (or when present, appear to be restricted to infratentorial regions). Given that the milder form of GAN presents like an axonal CMT-plus phenotype, with fewer systemic manifestations and without the MRI changes seen in the classic form, GAN should be included in next generation sequencing genetic platforms for CMT/hereditary neuropathies and should be classified as a form of axonal CMT-plus, while allowing for the possibility that as more patients are characterized, the upper motor neuron 'plus' features may be minimal or event absent. This may reduce the time to diagnosis, relieving the burden of the diagnostic odyssey for these patients and may also help expand the phenotype of GAN on the milder end of the spectrum, especially given a paucity of known adults with the milder GAN phenotype. Further studies to quantitatively assess functional, imaging, neurophysiological and biological markers in this milder GAN population, may allow us to better understand the long-term trajectory and prognosis of individuals with a phenotype along the milder spectrum of disease.

On comparative evaluation of quantitative motor and ambulatory abilities in individuals with GAN, we conclude that the MFM-32 percentage score represents an optimal composite scale to measure the decline in motor capacity secondary to the sensorimotor neuropathy, and that its functional subdomain percentage scores show differing trajectories of decline depending on the stage of disease. The total MFM-32 percentage score can distinguish subtle differences between individuals across various ages and levels of ambulatory function, and strongly cross-correlates across most of the other strength, timed testing, and neurophysiological measures (Fig. 4). Based on our cross-sectional and correlation data, we conclude that the MFM-32 serves as a highly suitable outcome measure that correlates to functional and electrophysiological measures of the disease and can be assessed across the spectrum of motor function and stage of disease in both the classic and the milder phenotype, and that other outcome measures or electrophysiological biomarkers tested may provide additional complementary information related to specific patterns of involvement. The MFM-32 scale has been analysed in cross-correlation as well as longitudinally in other neuromuscular disorders, such as in LAMA2-related dystrophy, COL6-related dystrophy and spinal muscular atrophy where annualized rates of decline have been predicted on the basis of longitudinal natural history studies.[37–39] Longitudinal data from future analysis in this study in GAN may determine whether the MFM-32 percentage score changes consistently over time, and whether its rate of change is
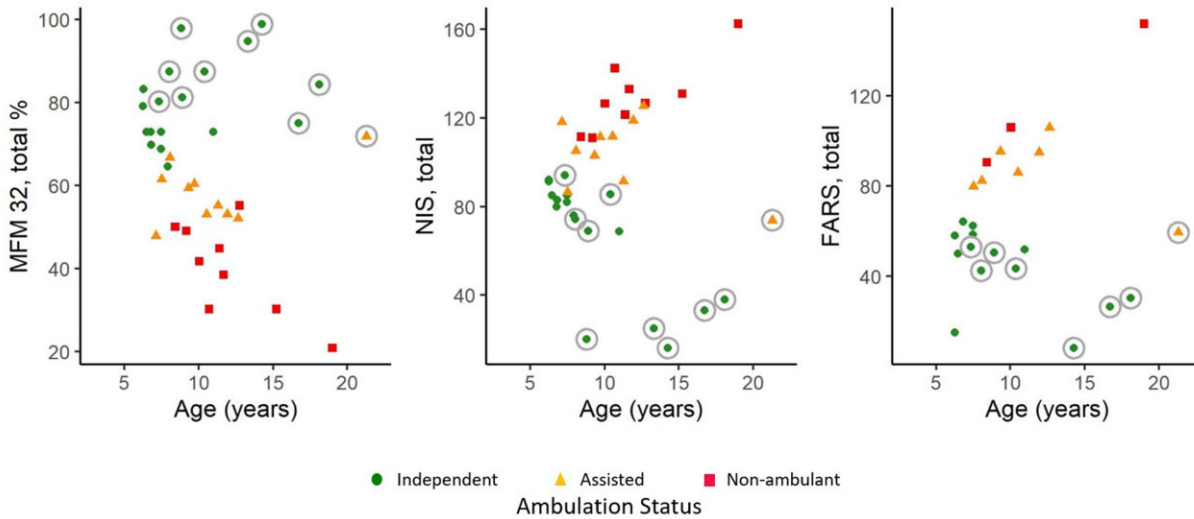
Figure 6 Composite/functional scores compared to age. Functional measures MFM-32 total percentage score, NIS and FARS are plotted by age and ambulation status. Functional outliers, or those with the milder GAN phenotype (*n* = 10), are denoted with grey circles. With milder GAN individuals (or functional outliers) excluded, there appears to be a more linear and homogeneous pattern between age and MFM-32, NIS and FARS amongst individuals with the classic phenotype.
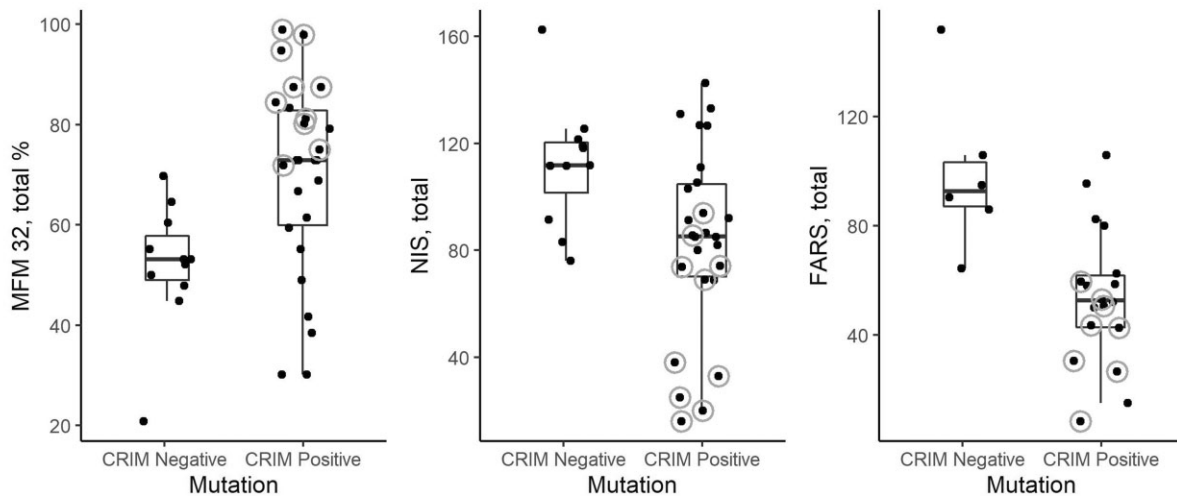
Figure 7 Impact of genetic subtype and milder GAN phenotype on functional assessments. Functional measures MFM-32 total percentage score, NIS and FARS plotted by mutation status. The box plots represent the 25th and 75th percentiles within each group, with whiskers defined as: upper limit: Q3 + 1.5 (IQR) or lower limit: Q1 − 1.5 (IQR). Predicted CRIM negative refers to those participants with biallelic null mutations. Functional outliers, or those with the milder GAN ('axonal CMT-plus') phenotype (*n* = 10), are denoted with grey circles. CRIM-negative participants do not ever manifest with the milder GAN phenotype, and on average tended to perform similar or slightly worse on functional scales compared to the CRIM-positive individuals, as demonstrated by a lower median MFM32 percentage score and higher median NIS and FARS score.

divergent between those with a classic versus milder GAN phenotype. Baseline clinical and functional data on the milder or axonal CMT-plus GAN patients would indicate the likelihood of a slower rate of progression as compared to the classic GAN phenotype. Additional functional rating scales such as the CMT Pediatric Scale or the CMT Neuropathy Score may be of increased relevance in the milder GAN population.

Baseline functional scales and assessments as well as review of medical history suggest that disease progression and the evolution of the neurological and non-neurological manifestations in the classic form of GAN tend to occur in a rather uniform and homogeneous manner. In contrast, the autonomic manifestations of the disease, such as abnormal sudomotor function measured by Q-

Sweat and the report of burden of autonomic features (COMPASS 31) in our series are present at younger ages and earlier in the disease, and thus do not appear to correlate with age or motor function (e.g. MFM-32 percentage score). While previous reports have noted clinical or pathological features that suggest the presence of autonomic dysfunction in individuals with GAN,[6,14,15] this is the first clinical study to systematically clinically evaluate a cohort of individuals with GAN for autonomic impairment. Clinical assessment for autonomic impairment as it may impact gastrointestinal, lacrimal, urinary, salivary and vasomotor function should be performed in the care of individuals with GAN. Follow-up studies such as quantitative evaluation of salivary function, gastrointestinal

motility and urinary function may further shed light on the severity and burden of autonomic dysfunction in individuals with GAN.

There was considerable heterogeneity as to the type and distribution of disease-causing variants throughout the GAN gene. In five individuals of Mexican descent with the classic phenotype of GAN we identified a recurrent homozygous splice-site mutation c.851+1G>A (IVS4+1G>A) in intron 4, suggesting a founder allele in this population. However, there is mutational heterogeneity in this population as the first GAN patient reported from Mexico was in fact compound heterozygous for two pathogenic variants in exon 9 and exon 11.[40] A different founder mutation c.1502+1G>T has been reported in the Turkish population.[41] In addition, we identified two confirmed and one suspected individual with GAN due to isodisomy (isoUPD). This is noteworthy in view of a previous report of an 18-year-old female with a homozygous splice-site variant, c.1237-1G>A on the basis of segmental maternal isoUPD.[42] The frequency with which isoUPD appears as a mutational mechanism in such an ultra-rare genetic disorder suggests that the genomic region of the GAN gene 16q23.2 may be prone to UPD. Confirming this, analysis of 205 UPDs identified in a population-based analysis of 916 712 Parent-Child 23andMe trios revealed that Chromosome 16 UPD is the most frequently observed UPD, followed by chromosomes 4, 1, 21, 22 and X and specifically, most are maternal greater than paternal UPD.[43] Biallelic predicted null variants were observed in 12/45 individuals, or 26.7% of this cohort. Individuals with such biallelic loss-of-function variants, who would be predicted to have absent gigaxonin expression (e.g. CRIM negative), all present with the classic GAN phenotype in contrast to individuals with the milder form of GAN who manifest with an axonal CMT-plus phenotype and who were all predicted to be CRIM positive. Therapeutic strategies such as gene replacement must take into account the need for adapting therapeutic strategies in CRIM-negative patients for whom the newly produced transgene protein, gigaxonin, may immunologically appear as foreign. In general, affected siblings or related individuals manifest similarly in disease features and trajectory, suggesting that intrafamilial phenotypic variability may not be prominent. This is in keeping with previous reports of similar phenotype and disease progression in multiple affected members of a kindred.[18,44]

While the cross-sectional data presented here allow for a powerful reconstruction of age dependent progression of the disease, our ongoing longitudinal analyses will help further refine the natural history of GAN by defining individual rates of progression clinically and quantitatively in the classic versus the milder GAN phenotypes. The existence of the milder phenotype of GAN, and its likely slower rate of disease progression, needs to be taken into account and defined longitudinally by key outcome measures, when used to plan and power ongoing as well as future clinical trials. Earlier and increasingly wide use of next generation sequencing based genetic testing platforms that include GAN will result in earlier diagnoses for individuals with GAN and should be prompted by clinical features including ataxia, distal weakness or axonal sensorimotor neuropathy, in particular when combined with tightly curled or curly hair. As gene-based therapeutic options are being explored, an early diagnosis will be essential to allow for timely intervention.

Acknowledgements

Funding

Competing interests

The authors report no competing interests.

Supplementary material

Supplementary material is available at *Brain* online.

References

1. Bomont P, Cavalier L, Blondeau F, et al. The gene encoding gigaxonin, a new member of the cytoskeletal BTB/Kelch repeat family, is mutated in giant axonal neuropathy. *Nat Genet*. 2000;26(3):370–374.

2. Koop O, Schirmacher A, Nelis E, et al. Genotype-phenotype analysis in subjects with giant axonal neuropathy (GAN). *Neuromusc Disord*. 2007;17(8):624–630.

3. Asbury AK, Gale MK, Cox SC, Baringer JR, Berg BO. Giant axonal neuropathy – A unique case with segmental neurofilamentous masses. *Acta Neuropath*. 1972;20(3):237–247.

4. Berg BO, Rosenberg SH, Asbury AK. Giant axonal neuropathy. *Pediatrics*. 1972;49(6):894–899.

5. Mussche S, De Paepe B, Smet J, et al. Proteomic analysis in giant axonal neuropathy: New insights into disease mechanisms. *Muscle Nerve*. 2012;46(2):246–256.

6. Johnson-Kerner BL, Ahmad FS, Garcia Diaz A, et al. Intermediate filament protein accumulation in motor neurons derived from giant axonal neuropathy iPSCs rescued by restoration of gigaxonin. *Hum Mol Genet*. 2015;24(5):1420–1431.

7. Kumar K, Barre P, Nigro M, Jones MZ. Giant axonal neuropathy: Clinical, electrophysiologic, and neuropathologic features in two siblings. *J Child Neurol*. 1990;5(3):229–234.

8. Perrot R, Eyer J. Neuronal intermediate filaments in neurodegenerative disorders. *Brain Res Bull*. 2009;80(4-5):282–295.

9. Pena SD, Opas M, Turksen K, Kalnins VI, Carpenter S. Immunocytochemical studies of intermediate filament aggregates and their relationship to microtubules in cultured skin fibroblasts from subjects with giant axonal neuropathy. *Eur J Cell Biol*. 1983;31(2):227–234.

10. Thomas C, Love S, Powell HC, Schultz P, Lampert PW. Giant axonal neuropathy: Correlation of clinical findings with post mortem neuropathology. *Ann Neurol*. 1987;22(1):79–84.

11. Yang Y, Allen E, Ding J, Wang W, Human G, Diseases R. Giant axonal neuropathy. *Cell Mol Life Sci*. 2007;64(5):601–609.

12. Incecik F, Herguner OM, Ceylaner S, Zorludemir S, Altunbasak S. Giant axonal disease: Report of eight cases. *Brain and Development*. 2015;37(8):803–807.

13. Nalini A, Gayathri N, Yasha TC, et al. Clinical, pathological and molecular findings in two siblings with giant axonal neuropathy (GAN): Report from India. *Eur J Med Gen*. 2008;51(5):426–435.

14. Gambarelli D, Hassoun J, Pellissier JF, Livet MO, Pinsard N, Toga M. Giant axonal neuropathy. Involvement of peripheral nerve, myenteric plexus and extra-neuronal area. *Acta Neuropathol*. 1977;39(3):261–269.

15. Armao D, Bailey RM, Bouldin TW, Kim Y, Gray SJ. Autonomic nervous system involvement in the giant axonal neuropathy (GAN) KO mouse: Implications for human disease. *Clin Auton Res*. 2016;26(4):307–313.

16. Almeida HL, Garcias G, Silva RM, Batista SL, Pasetto F. Pili canaliculi as manifestation of giant axonal neuropathy. *Na Bras Dermatol*. 2016;91(5 Suppl 1):125–127.

17. Roth LA, Marra JD, LaMarca NH, Sproule DM. Measuring disease progression in giant axonal neuropathy: Implications for clinical trial design. *J Child Neurol*. 2015;30(6):741–748.

18. Abu-Rashid M, Mahajnah M, Jaber L, et al. A novel mutation in the GAN gene causes an intermediate form of giant axonal neuropathy in an Arab-Israeli family. *Eur J Paediatric Neurology*. 2013;17(3):259–264.

19. Brenner C, Speck-Martins CE, Farage L, Barker PB. 3T MR with diffusion tensor imaging and single-voxel spectroscopy in giant axonal neuropathy. *J Magn Reson Imaging*. 2008;28(1):236–241.

20. Vijaykumar K, Bindu PS, Taly AB, et al. Giant axonal neuropathy. *J Child Neurol*. 2015;30(7):912–915.

21. Koichihara R, Saito T, Ishiyama A, et al. A mild case of giant axonal neuropathy without central nervous system manifestation. *Brain Dev*. 2016;38(3):350–353.

22. Tazir M, Nouioua S, Magy L, et al. Phenotypic variability in giant axonal neuropathy. *Neuromusc Disord*. 2009;19(4):270–274.

23. Xu M, Da Y, Liu L, Wang F, Jia J. Giant axonal neuropathy caused by a novel compound heterozygous mutation in the gigaxonin gene. *J Child Neurol*. 2013;28(10):1316–1319.

24. Aharoni S, Barwick KES, Straussberg R, et al. Novel homozygous missense mutation in GAN associated with Charcot-Marie-Tooth disease type 2 in a large consanguineous family from Israel. *BMC Med Genet*. 2016;17(1):82–88.

25. Sletten D, Grandinetti A, Weigand S, et al. Normative values for sudomotor axon reflex testing using QWEAT. *Neurology*. 2015;84: P1.282.

26. Saal DP, Thijs RD, Van Dijk JG. Tilt table testing in neurology and clinical neurophysiology. *Clin Neurophysiol*. 2016;127(2): 1022–1030.

27. Dyck PJ, Boes CJ, Mulder D, et al. History of standard scoring, notation, and summation of neuromuscular signs. A current survey and recommendation. *J Peripher Nerv Syst*. 2005;10(2): 158–173.

28. Burk K, Schulz SR, Schulz JB. Monitoring progression in Friedreich ataxia (FRDA): The use of clinical scales. *J Neurochem*. 2013; 126 (Suppl 1): 118–124.

29. Berard C, Payan C, Hodgkinson I, Fermanian J. A motor function measure for neuromuscular diseases. Construction and validation study. *Neuromusc Disord*. 2005;15(7):463–470.

30. Vuillerot C, Rippert P, Kinet V, et al.; CDM MFM Study Group. Rasch analysis of the motor function measure in patients with congenital muscle dystrophy and congenital myopathy. *Arch Phys Med Rehabil*. 2014;95(11):2086–2095.

31. Nagy S, Schmidt S, Hafner P, et al. Measures of motor function and other clinical outcome parameters in ambulant children with Duchenne muscular dystrophy. *J Vis Exp*. 2019;(143): e58784.

32. Waite M, Bharucha-Goebel D, Moulton T, et al. Comparison of two clinical motor scales in individuals with giant axonal neuropathy (GAN). *Neuromusc Disord*. 2015;25:S284–S285.

33. Pierangeli G, Turrini A, Giannini G, et al. Translation and linguistic validation of the composite autonomic symptom score COMPASS 31. *Neurol Sci*. 2015;36(10):1897–1902.

34. Chidi-Egboka NC, Briggs NE, Jalbert I, Golebiowski B. The ocular surface in children: A review of current knowledge and meta-analysis of tear film stability and tear secretion in children. *Ocul Surf*. 2019;17(1):28–39.

35. Ries M, Gupta S, Moore DF, et al. Pediatric Fabry disease. *Pediatrics*. 2005;115(3):e344–355.

36. Staiano A, Santoro L, De Marco R, et al. Autonomic dysfunction in children with Hirschsprung's Disease. *Dig Dis Sci*. 1999;44(5):960–965.

37. Vuillerot C, Payan C, Iwaz J, Ecochard R, Bérard C. and.;MFM Spinal Muscular Atrophy Study Group. the MFM Spinal Muscular Atrophy Study Group. *Arch Phys Med Rehab*. 2013;94(8):1555–1561.

38. Chabanon A, Seferian AM, Daron A, et al. ;NatHis-SMA study group. Prospective and longitudinal natural history study of patients with Type 2 and 3 spinal muscular atrophy: Baseline data NatHis-SMA study. *PLoS ONE*. 2018;13(7):e0201004.

39. Jain MS, Meilleur K, Kim E, et al. Longitudinal changes in clinical outcome measures in COL6-related dystrophies and LAMA2-related dystrophies. *Neurology*. 2019;93(21):e1932–e1943.

40. Normendez-Martínez MI, Monterde-Cruz L, Martínez R, et al. Two novel mutations in the GAN gene causing giant axonal neuropathy. *World J Pediatr*. 2018;14(3):298–304.

41. Edem P, Karakaya M, Wirth B, Okur TD, Yis U. Giant axonal neuropathy: A differential diagnosis of consideration. *Turk J Pediatr*. 2019;61(2):275–278.

42. Miyatake S, Tada H, Moriya S, et al. Atypical giant axonal neuropathy arising from a homozygous mutation by uniparental isodisomy. *Clin Genet*. 2015;87(4):395–397.

43. Nakka P, Pattillo Smith S, O'Donnell-Luria AH, et al.; 23andMe Research Team. Characterization of prevalence and health consequences of Uniparental Disomy in four million individuals from the general population. *Am J Hum Genet*. 2019;105(5): 921–932.

44. Zemmouri R, Azzedine H, Assami S, et al. Charcot-Marie-Tooth 2-like presentation of an Algerian family with giant axonal neuropathy. *Neuromusc Disord*. 2000;10(8):592–598.

45. Beenakker EAC, Van der Hoeven JH, Fock JM, Maurits NM. Reference values of maximum isometric muscle force obtained in 270 children aged 4-16 years by hand-held dynamometry. *Neuromuscl Disord*. 2001;11(5):441–446.

46. Annoussamy M, Lilien C, Gidaro T, et al. X-linked myotubular myopathy: A prospective international natural history study. *Neurology*. 2019;92(16):e1852–e1867.

47. Gontier J, Fisch U. Schirmer's Test: Its normal values and clinical significance. *J Otorhinolaryngol Relat Spec*. 1976;38(1):1–10.